

# Polymeric Nanospheres with Tunable Sizes, Water Dispersibility, and Thermostability from Heating-Enabled Micellization of Polysulfone-*Block*-Polyethylene Glycol

Zexian Zhang,<sup>1†</sup> Jie Li,<sup>2†</sup> Zhaogen Wang,<sup>2</sup> Changcheng He,<sup>1</sup> Yong Wang <sup>2</sup>

<sup>1</sup>Beijing Key Laboratory of Energy Conversion and Storage Materials, College of Chemistry, Beijing Normal University, Beijing 100875, People's Republic of China

<sup>2</sup>State Key Laboratory of Materials-Oriented Chemical Engineering, College of Chemical Engineering, Nanjing Tech University, Nanjing, Jiangsu 210009, People's Republic of China

Correspondence to: C. He (E-mail: herbert@bnu.edu.cn) or Y. Wang (E-mail: yongwang@njtech.edu.cn)

Received 21 December 2017; accepted 8 February 2018; published online 12 March 2018

DOI: 10.1002/polb.24596

**ABSTRACT:** Polymeric nanospheres with uniform sizes, functional surfaces, and high mechanical strength and thermostability are attracting wide interest in different applications. Here, a new kind of polysulfone micellar spheres with PEGylated surfaces is prepared via directly heating the solution of an amphiphilic block copolymer, polysulfone-*b*-polyethylene glycol (PSF-*b*-PEG). The sizes of the micelles are uniform and tunable between ~42 and ~443 nm. TEM characterizations show that the micelles are core-shell structures with PEG as the corona and PSF as the core. PEG endows the micelles with dispersibility in water and good biocompatibility, while PSF provides the mechanical strength and thermostability. The effects of PEG

contents, polymer solution concentrations, solvent types, and heating temperatures are systematically investigated. Furthermore, heat resistance tests show that the micelles are stable at 150–180 °C. These PSF-*b*-PEG micellar spheres are expected to be applied in demanding environmental conditions such as heating involved surface modification process. © 2018 Wiley Periodicals, Inc. *J. Polym. Sci., Part B: Polym. Phys.* **2018**, *56*, 769–777

**KEYWORDS:** micellization; nanospheres; polyethylene glycol; polysulfone; thermostability

**INTRODUCTION** Polymeric nanospheres are receiving increasing scientific attention in many fields ranging from nanotechnology to drug delivery.<sup>1,2</sup> As a typical kind of polymeric nanospheres, spherical polymeric micelles are of great interest due to their large specific surface area, high diffusibility and mobility, and unique core-shell nanostructures.<sup>3,4</sup> Many strategies have been explored for the preparation of spherical micelles, among which the amphiphilic block copolymer (BCP) micellization route is distinguished because of the advantages such as uniform pore sizes and functionalizable surfaces.<sup>5</sup> BCPs are a group of polymers linked by covalent bonds of two or more blocks with different chemical properties.<sup>6</sup> They can self-assemble into polymeric micelles in dilute solutions, which have been widely studied.<sup>5</sup> Different nanoaggregates such as spherical micelles, nanotubes vesicles, wormlike aggregates, and complex micelles can be formed via the self-assembly behavior of amphiphilic BCPs in selective solvents.<sup>7–9</sup> During the preparation of micelles,

polar solvents are generally used as the selective solvents. If BCP is dissolved in a nonpolar solvent, reverse micelles may be formed.<sup>9–11</sup> However, the applications of reverse micelles are much limited due to their poor dispersibility in aqueous conditions.<sup>12</sup>

There are two processes affecting the preparation of spherical micelles using amphiphilic BCPs, one is the physical interaction starting from synthetic or natural polymers and another is different particle-forming polymerization starting from monomers.<sup>13,14</sup> Accordingly, the morphologies of the BCP micelles can be controlled by changing the molecular parameters (such as repeating structure units and molecular weight of the segments) and solution parameters (such as solvents, concentration, temperature, additives, etc.).<sup>15</sup> For instance, Cho studied the effect of molecular weight on the size of polystyrene-*block*-poly(2-vinyl pyridine) (PS-*b*-P2VP) nanoparticles and found that stable nanospheres with diameter

<sup>†</sup>These authors contributed equally to this work.

Additional Supporting Information may be found in the online version of this article.

© 2018 Wiley Periodicals, Inc.

<100 nm can be obtained by controlling molecular weights.<sup>16</sup> The effects of the hydrophilic and hydrophobic block lengths and different ions on the morphology and micelle core and corona of polystyrene-*block*-poly(acrylic acid) (PS-*b*-PAA) were also investigated.<sup>17,18</sup> To be noted, fluorescence can also be introduced to BCP micelles to expand their applications.<sup>19</sup> One common strategy to prepare BCP micellar spheres involves a two-step process. In this process, BCPs are firstly dissolved in a good solvent for both blocks and then a selective solvent for one of the blocks is gradually added to induce micellization. This strategy is efficient in producing micelles with different structures.<sup>16–18</sup> Nevertheless, most of the processes are somewhat tedious and time-consuming. Moreover, because different phases corresponding to specific morphologies normally occupy a relatively narrow region in the phase diagram of BCPs, other structures (e.g., cylinders or vesicles) frequently coexist among the obtained spheres, which practically contaminate the purity of the final micellar products. Therefore, a simple, one-step micellization process able to exclusively produce spherical micelles is highly demanded. Alternatively, we applied one-step heating-enabled micellization to the preparation of monodisperse PS-*b*-P2VP nanospheres.<sup>20</sup> Water-dispersed PS-*b*-P2VP nanospheres with chromophores residing in the cores were obtained by dissolving PS-*b*-P2VP together with chromophores (perylene and pyrene) in acetic acid at elevated temperatures. This direct dissolution method is of great simplicity and capable of exclusively producing spherical micelles, especially for BCPs with a long glassy, hydrophobic block, and short hydrophilic chains. The nanospheres can be used as a probe to characterize pore sizes of separating membranes and detect large-pore defects.<sup>21</sup>

However, most of the above BCP nanospheres are suffering from poor mechanical robustness, thermal stability, and relatively high cost, which limit their applications. For instance, PS nanospheres can hardly bear temperatures higher than the glass transition temperature of PS, namely,  $\sim 100$  °C.<sup>22</sup> Therefore, polymeric nanospheres with functional surfaces, high mechanical strength, and thermostability are highly desired.

Polysulfone (PSF) consisting of alkyl-sulfonyl-arylene chains is widely used in industry. PSF materials are relatively inexpensive and able to withstand many harsh processes. Due to the presence of sulfur atoms with the highest oxidation state and the highly conjugated arylene structure in the polysulfone, PSF has excellent oxidation resistance and thermal stability. Besides, the benzene ring in the chain improves the mechanical strength of PSF, and the ether bond improves the ductility of PSF, so PSF is resistant to acid, alkali, and hydrolysis.<sup>23</sup> Despite the excellent chemical, thermal, and mechanical stability of PSF, rare works have been reported for the development of PSF-based micelles. To fill the blank, herein, we choose PSF as the hydrophobic segment in the attempt to prepare BCP micelles with high mechanical strength and thermostability. To improve the hydrophilic nature of PSF materials, polyethylene glycol (PEG) is chosen as the

hydrophilic segment, that is, polysulfone-*b*-polyethylene glycol (PSF-*b*-PEG) is used. In this work, we demonstrate, for the first time, the preparation of PSF-*b*-PEG micellar nanospheres via the direct dissolution route in a selective solvent. TEM was used to observe the spherical shell structure and phase distribution of the PSF-*b*-PEG micelles, which were stained with a hydrophilic dye osmium tetroxide. A systematic study of the effects of the solvent, PEG content, temperature, and concentration on the particle size and morphology of the micelles was carried out. Furthermore, we investigated the high temperature resistance and the dispersibility in water of the micellar nanospheres, which lay the foundation for the application of the nanospheres in high temperature environment and in water environment.

## EXPERIMENTAL

### Materials

PSF-*b*-PEG block copolymers were obtained from Nanjing Bangding. According to the manufacturer, the copolymers had a similar PEG molecular weight ( $M_w$ ) of  $\sim 20$  kDa and varying PSF molecular weights. The polydispersive index (PDI) was  $\sim 2.00$ . PS-*b*-P2VP ( $M_n$  (PS) = 55 kDa,  $M_n$  (P2VP) = 18.5 kDa) was purchased from Polymer Source Inc., Canada. Ethanol (AR grade) was purchased from Sinopharm Chemical Reagent Co., Ltd. (Beijing, China) and acetic acid (AR grade) was purchased from Shanghai Shenbo Chemical Co., Ltd. (Shanghai, China).

### Preparation of Micelles

When the temperature for micellization was lower than the boiling point of the selective solvent, a 25-mL glass bottle with a plastic cover was used as the container for better observation. We mixed PSF-*b*-PEG with the solvent (acetone or acetic acid (AA)) at a weight percentage of 0.01–5 wt % in the capped bottle and then transferred the mixture into an oven heated at certain temperatures (55 °C for acetone, 110 °C for AA) for  $\sim 5$  min. After that, we took out the glass bottle, loosened the cap to release the solvent vapor accumulated by heating, and then continued the heating process for  $\sim 5$  min. This procedure should be repeated 3 times, during which PSF-*b*-PEG was gradually dissolved, forming a milky solution. After a total heat treatment for certain durations (6 h for acetone and 24 h for AA), the glass bottle was removed from the oven and cooled to room temperature. The obtained micellar solutions were kept for later characterizations and tests. When the temperature for micellization was higher than the boiling point of the selective solvent, a stainless-steel autoclave with a polytetrafluoroethylene inner liner was used as the container. PSF-*b*-PEG was mixed with AA, heated at certain temperatures (150 °C and 180 °C) for 24 h, and then taken out from the oven. No loosening procedure was needed. PS-*b*-P2VP micelles were prepared by heated in 110 °C AA for 5 h.

### Characterizations

The PSF-*b*-PEG samples which had been dried adequately were performed on a thermogravimetry (TG) analyzer (449F,

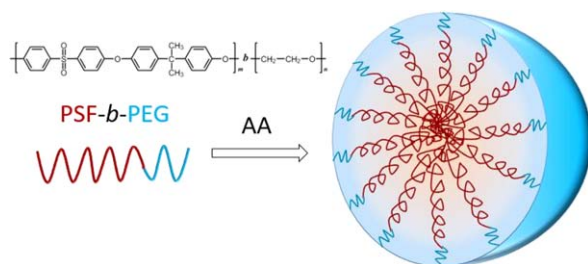


**FIGURE 1** The schematic diagram of the formation of PSF-*b*-PEG spherical micelle with core-shell structure through direct dissolving method. [Color figure can be viewed at wileyonlinelibrary.com]

TA Instruments, USA) at heating rate of 10 °C/min under nitrogen atmosphere, with the temperature ranging from room temperature to 800 °C. We diluted 0.01 wt % BCP micellar solutions with the same solvent for 100- to 500-fold for scanning electron microscopy (SEM-S4800, Hitachi Co., Ltd., Japan) and transmission electron microscopy (TEM-Tecnaï 12, Philips Co., Ltd., Netherlands) examination. The diluted PSF-*b*-PEG micellar solutions were dripped on silicon wafer shards or carbon-coated copper grids for SEM and TEM examination, respectively. The silicon wafer containing micellar solutions was placed in the air dry oven at 50 °C for 3 h and was SEM tested at 5 keV after sputter coating a thin layer of gold. TEM images were operated at 300 keV. For all micelles, we exposed the micelles deposited on copper grids to osmium tetroxide vapor at room temperature for 12 h to selectively adhere to the PEG domains prior to TEM probing. The PSF-*b*-PEG spherical micelles prepared in acetic acid were separated by centrifugation, and then the obtained solid powders were exposed in deionized water by 30 min ultrasonic to ensure the full dispersion of the micelles. The dynamic light scattering (DLS) curves were recorded on a Zetatracc particle size analyzer (ZS90, Malvern Instruments Co., Ltd., UK).

## RESULTS AND DISCUSSION

According to our previous study, nanospherical micelles of amphiphilic PS-*b*-P2VP with PS as the core and P2VP as the corona could be formed in a polar solvent such as acetic acid (AA).<sup>20</sup> Similarly, in this work, PSF-*b*-PEG amphiphilic nanospherical micelles with PSF as the core and PEG as the shell are prepared by heating-enabled micellization in polar solvents, and the sizes of the micelles can be effectively controlled by block ratio, solvent, temperature, and so on. The hydrophilic difference and thermodynamic incompatibility between the PSF block and PEG block leads to microphase separation of PSF-*b*-PEG, thus solid nanospheres are produced in AA. As the hydrophobic BCP block is a long chain segment with high glass transition temperature ( $T_g$ ), the micelles show a morphology of hard crew-cut nanospheres. Here, the heating process is conducted to enhance the affinity between the hydrophilic PEG segments and AA, thus promoting their movements in AA and ensuring the forming of rigid and homogeneous nanospheres (Fig. 1).

## Thermogravimetric Analysis of PSF-*b*-PEG

PEG contents of the PSF-*b*-PEG samples can be obtained by TG analyses. Thermal degradation of PSF-*b*-PEG can be divided into two steps. The degradation temperature of PEG and PSF block is 385.5 °C and higher than 450 °C, respectively.<sup>24</sup> Therefore, the thermal decomposition of PEG block will occur first, and PSF decomposition is followed during the whole heating process. Figure 2 shows the TG curves of different batches of PSF-*b*-PEG. According to the TG curve, we can calculate the loss percentage resulting from the degradation of PEG block, thus the content of PEG block in PSF-*b*-PEG can be worked out. The content of PEG in FG-1, FG-2, FG-3, and FG-4 is 14%, 21%, 31%, and 47%, respectively. From the TG curves, we can find that the final mass loss is not zero. The residual mass comes from the PSF-*b*-PEG carbonization in nitrogen atmosphere. The TG analysis provides the data basis for the selection of copolymers with different PEG contents in subsequent experiments.

## Structures of PSF-*b*-PEG Micelles

We investigated the heating-enabled micellization of PSF-*b*-PEG with the PEG content of 47% (FG-4) first. TEM characterizations demonstrated the spherical morphology of the particles and showed the particles had a solid interior. To verify the location and distribution of PSF block and PEG block, we exposed the PSF-*b*-PEG nanospheres on a copper grid to osmium tetroxide (OsO<sub>4</sub>) vapor at room temperature for 12 h. The TEM image is shown in Figure 3. Because osmium tetroxide was selectively absorbed on the PEG block,<sup>25</sup> the spheres possessed the thin darker corona of PEG and the thick gray core of PSF. The diameter of spherical micelles was determined to be 130 nm and the thickness of the PEG corona was 12 nm. By calculation, it can be got that the volume of the shell is ~46% of the sphere, which is basically consistent with the 47% PEG content by TG tests.

## Solvent Selection for the Micellization of PSF-*b*-PEG

PSF-*b*-PEG (FG-1, whose PEG block content is 14%) was dissolved in acetone and AA, respectively. Figure 4 shows the

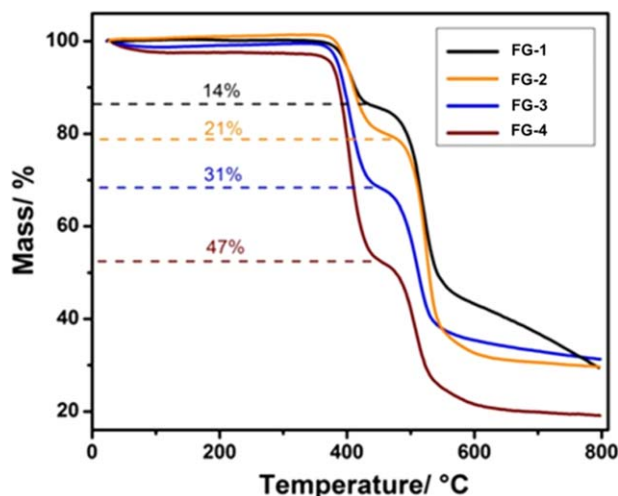


**FIGURE 2** TG curves of different batches of PSF-*b*-PEG. [Color figure can be viewed at wileyonlinelibrary.com]

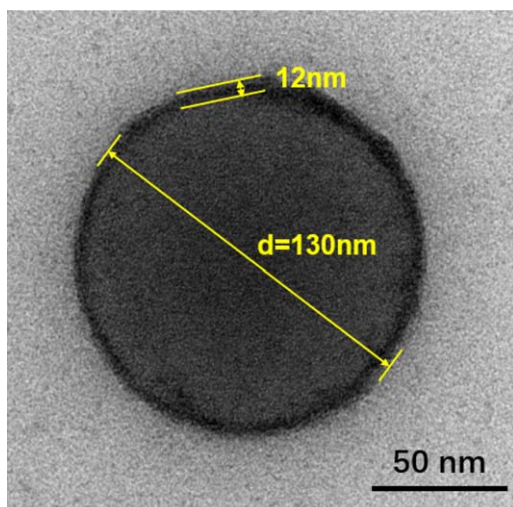


**FIGURE 3** TEM image of the FG-4 micelle after stained with  $\text{OsO}_4$ . [Color figure can be viewed at [wileyonlinelibrary.com](http://wileyonlinelibrary.com)]

SEM images of the FG-1 micelles and the corresponding size distribution histograms in different solvents. Spherical micelles can be obtained at 55 °C for 6 h using acetone as the solvent or heated at 150 °C for 24 h in autoclave using AA as the solvent. From the SEM images, we calculated the average size of the particles in acetone (156 nm) and in AA (136 nm). As a result of the strong acid–base interaction

between the carboxylic groups of AA and hydroxyl of PEG, AA shows better affinity toward PEG. Therefore, the sizes of the micelles obtained using AA as solvent are more uniform than those of spherical micelles obtained from acetone. So AA was used as the polar solvent in the subsequent experiments. We note that the micelles prepared in AA are also not very uniform in diameter due to the relatively high PDI ( $\sim 2.00$ ) of the PSF-*b*-PEG block copolymers. In addition, as PEG with a molecular weight of  $\sim 20$  kDa is highly crystallizable, we expect that the micellar corona composed of PEG is crystalline while the PSF micellar core should keep amorphous because the micellization process is not likely to change the amorphous nature of PSF.

#### Effects of Block Ratio on the Micellization of PSF-*b*-PEG

Previous study showed that the nuclear layer radius ( $R_c$ ) of the BCP micelle is dependent on the polymerization degree of hydrophobic chains ( $N_B$ ) and the degree of polymerization of the hydrophilic chains ( $N_A$ ). The quantitative relationship is as follows<sup>17</sup>:

$$R_c \propto N_B^\alpha N_A^{-\gamma} (0.67 \leq \alpha \leq 0.76, 0 \leq \gamma \leq 0.1) \quad (1)$$

Longer hydrophobic chains will lead to the aggregation of more copolymer molecules and consequently higher  $R_c$  value. We dissolved FG-4, FG-3, FG-2 and FG-1 (the PEG content was 47%, 31%, 21%, and 14%, respectively) in AA with the solution concentration of 0.01 wt % and kept the solutions

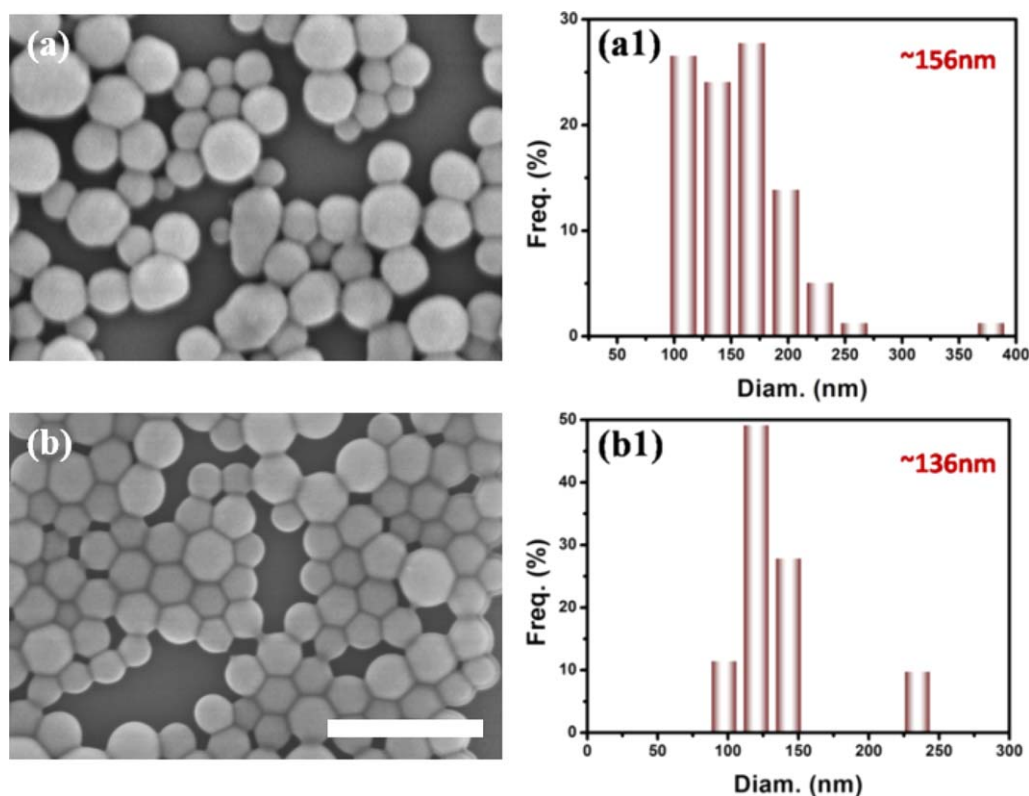


**FIGURE 4** SEM images of the FG-1 micelles and the corresponding size distribution histograms in different solvents: (a), (a1) acetone; (b), (b1) acetic acid. (a) and (b) have the same magnification and the scale bar in (b) is 500 nm. [Color figure can be viewed at [wileyonlinelibrary.com](http://wileyonlinelibrary.com)]

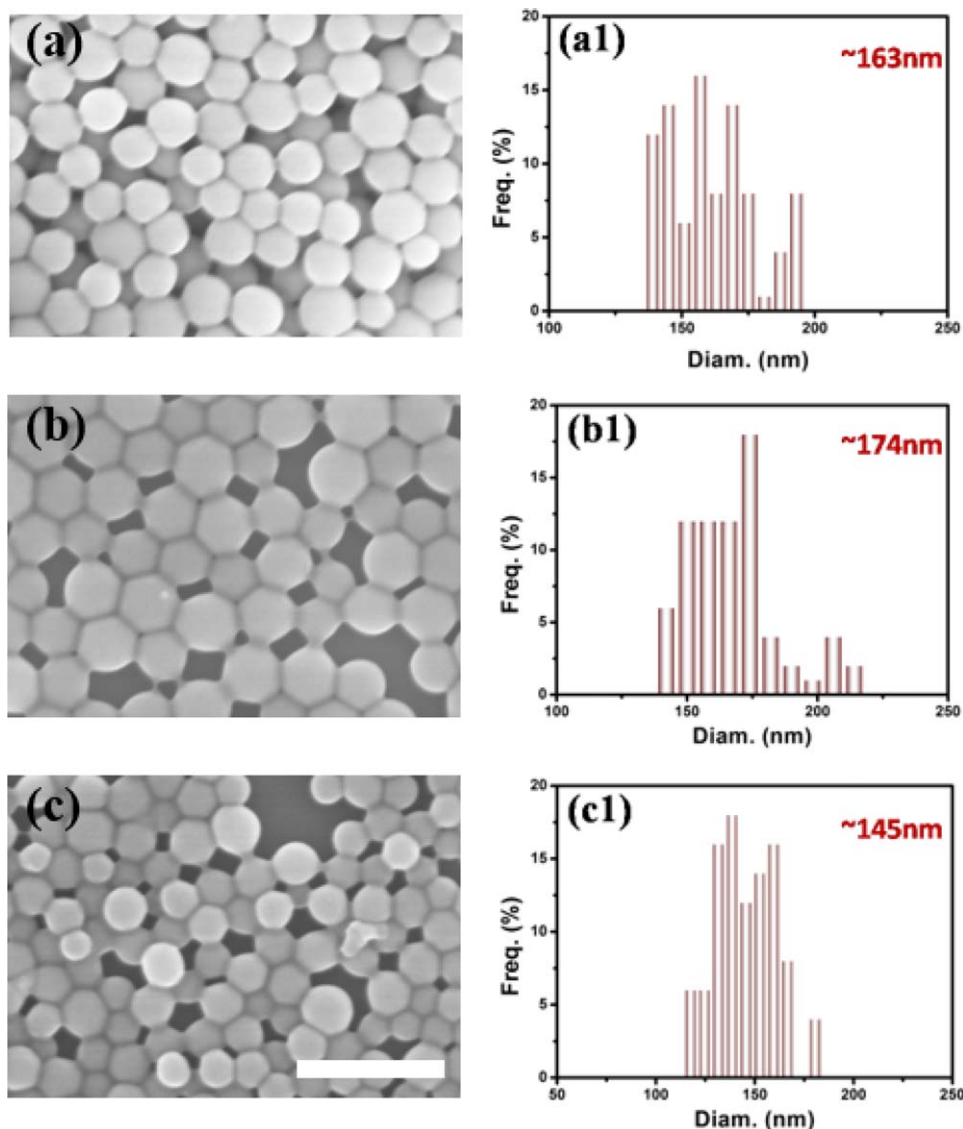


**FIGURE 5** SEM images of the PSF-*b*-PEG micelles with different PEG block ratios: (a) FG-4 (47%); (b) FG-3 (31%); (c) FG-2 (21%). (a1, b1, c1) are the corresponding size distribution histogram with different PEG block ratios. (a), (b), and (c) have the same magnification and the scale bar in (c) is 500 nm. [Color figure can be viewed at [wileyonlinelibrary.com](http://wileyonlinelibrary.com)]

in autoclave at 150 °C for 24 h, respectively. Figure 4(b) and 5 show the SEM images and DLS results. We can find that the sizes of the spherical micelles basically decrease with the decrease of PEG content, and the size of dry micelles is 163 nm (FG-4), 174 nm (FG-4), 145 nm (FG-4), and 135 nm (FG-4), respectively. The tendency of the size of dry micelles seems not consistent with that predicted by formula (1). This is because Equation 1 describes the nuclear layer (micellar core) radius rather than the radius of the whole sphere of the micelle. In fact, the influence of the PEG block on micelle size cannot be neglected,<sup>26</sup> and higher PEG contents will lead to higher thickness of the micellar shell.

#### Effects of Temperature on the Micellization of PSF-*b*-PEG

Temperature is one of the most important factors affecting the heating-induced micellization process. We dissolved FG-

2 and FG-4 in AA to prepare polymer solutions ( $C = 0.1$  wt %) and kept the solutions at 110 °C, 150 °C, and 180 °C for 24 h, respectively. Figure 6 and Supporting Information, Figure S1 show the SEM images of FG-4 and FG-2 micelles prepared in AA of different temperatures. From the SEM images, it can be assured that spherical micelles can be prepared taking advantages of the both samples, and the size of the micelles increases with the increase of the temperature. For instance, as to FG-4 is concerned, when it was heated at 110, 150, or 180 °C, the diameter of the obtained micelles was 42, 282, and 443 nm, respectively. It is very clear that the size of spherical micelles increases with the increase of the temperature. For FG-2, the spherical morphology of the micelles disappeared at 110 °C, indicating that there exists a critical temperature for the micellization behavior, and the critical temperature was below 110 °C.

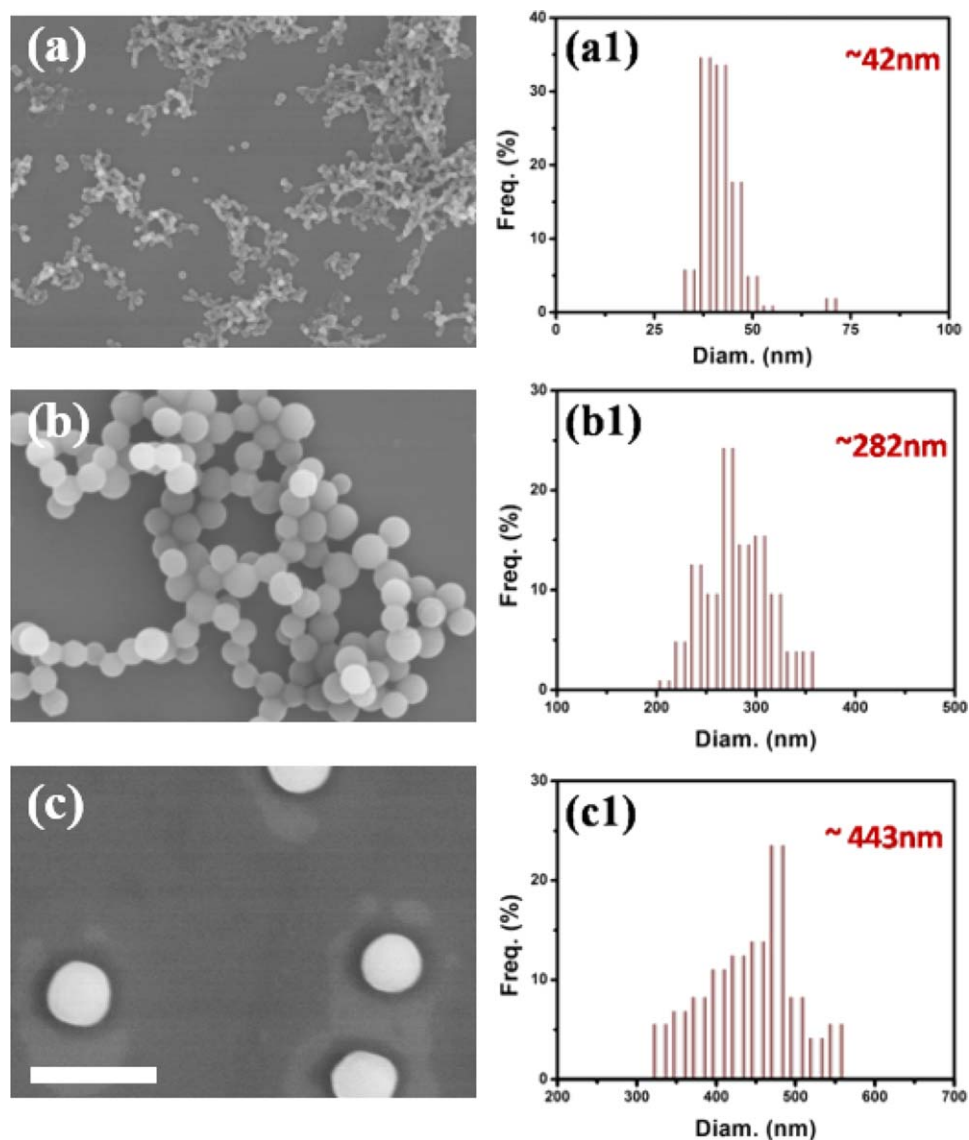


**FIGURE 6** SEM images of the FG-4 micelles prepared in AA at different temperatures: (a) 110 °C; (b) 150 °C; (c) 180 °C. (a1, b1, c1) are the corresponding size distribution histogram in 110 °C, 150 °C, and 180 °C. (a), (b), and (c) have the same magnification and the scale bar in (c) is 1000 nm. [Color figure can be viewed at [wileyonlinelibrary.com](http://wileyonlinelibrary.com)]

Below this critical temperature, it is difficult to obtain spherical micelles.

The increase of temperature does good to increase the affinity between the blocks and the solvent. The affinity is characterized by the polymer-solvent interaction parameter (Huggins parameter,  $\chi_{P-S}$ ), which can be estimated by the van Laar-Hildebrand equation,<sup>20</sup>

$$\chi_{P-S} = V_S / (RT) \times (\delta_P - \delta_S)^2 \quad (2)$$

where  $V_S$  is the molar volume of the solvent and  $\delta_P$  and  $\delta_S$  are solubility parameters of the polymer and the solvent, respectively. Generally, the effects of temperature to  $V_S$ ,  $\delta_P$  and  $\delta_S$  are neglectable. Equation 2 shows that the value of  $\chi_{P-S}$  decrease with the increase of temperature, suggesting the solubility of

polymers in solvents is promote.<sup>20</sup> In addition, the increase of temperature also enhances the mobility of the segments, the occurrence of the aggregation of the chain segments is accelerated and the micelles are easier to bend to form the cores or corona in the micellization process. So, the size of the micelles increases with the increase of temperature.

#### Effects of Solution Concentration on the Micellization

We dissolved FG-4 in AA with the solution concentration of 0.01, 0.1, 1, 3, and 5 wt %, respectively, and placed the solutions in autoclave, then kept the autoclave in vacuum drying oven at 150 °C for 24 h. The obtained BCP micellar solutions were dropped on silicon wafer shards for SEM observations.

As shown in Supporting Information, Figure S2, when the concentrations of PSF-*b*-PEG solutions change from 0.01 to

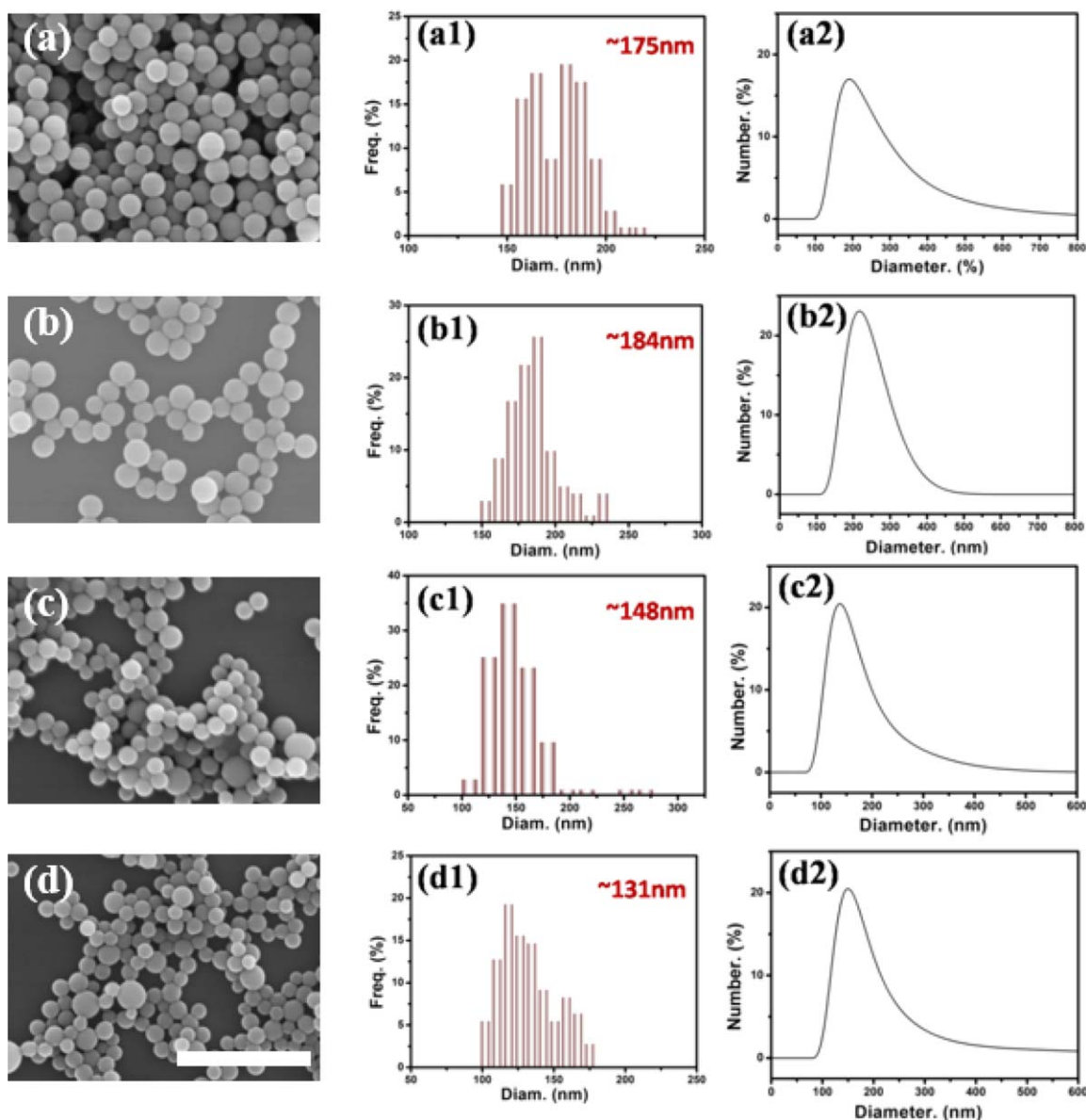


**FIGURE 7** SEM images of the PSF-*b*-PEG micelles with different PEG block ratio dispersed in deionized water: (a) FG-4; (b) FG-3; (c) FG-2; (d) FG-1. (a1, b1, c1, d1) are the corresponding size distribution histogram. (a2, b2, c2, d2) are the DLS curves of the micelles. (a), (b), (c), and (d) have the same magnification and the scale bar in (d) is 1000 nm. [Color figure can be viewed at [wileyonlinelibrary.com](http://wileyonlinelibrary.com)]

0.1 wt %, the micelle size increases from 145 to 252 nm, which then reduces to 94 nm when the concentration increases to 1 wt %. With the concentration increased to 3 and 5 wt %, the diameter of the micelles is 85 and 82 nm, respectively. Obviously, the solution concentrations have an influence on the particle sizes of micelles. With the increase of solution concentration, the size of the micelle increases firstly. When the particle size reached the maximum value, it decreases and finally remains unchanged. There seems to be one critical value of concentration in the preparation of PSF-*b*-PEG micelles. When the BCP concentration is relatively low, the aggregation number of the micelles will increase with higher concentrations, which makes the final micelles

larger. As the BCP concentration increases to the critical value, the mobility of the chain segments is suppressed and the aggregation number decreases,<sup>6</sup> leading to smaller micelle size. When the concentration is further increased, the micelle size will tend to be unchanged.

#### Dispersivity of the Micelles in Water

The PSF-*b*-PEG micelle solutions (1 wt %) were centrifuged to obtain the final solid powders, which were subsequently dried in a 60 °C drier. As the obtained solid powders were spherical micelles with PSF as the core and PEG as the corona, they should be well dispersed in water. After the dried solid powders were solute using deionized water as

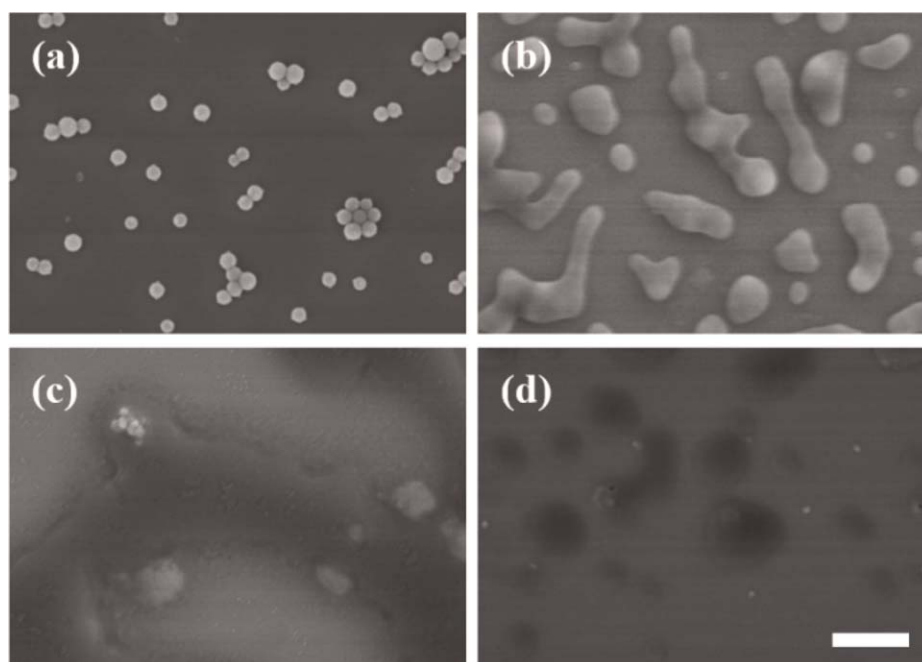


**FIGURE 8** SEM images of the FG-2 micelles after treatment at (a) 150 °C, (b) 180 °C, and (c) 200 °C for 30 min, respectively. (d) is the FG-4 micelles after treatment at 150 °C for 30 min. (a), (b), (c), and (d) have the same magnification and the scale bar in (d) is 1000 nm.

solvent and 10 min treated by ultrasonic, the micelles were well dispersed. Then the solutions were characterized by SEM and DLS. As shown in Figure 7, the micelles show a single particle size distribution peak, thus it can be concluded that micelles have narrow size distribution and good dispersion in water. In dry state, the particle size is 175, 184, 148, and 131 nm corresponded to FG-4, FG-3, FG-2, and FG-1, respectively (PEG content is 47%, 31%, 21%, and 14%), while the size of micelles under wet state is 190, 210, 160, and 149 nm, respectively. In water, the PEG segments of the micelle shell are in a swollen state, and the sizes of the micelles become larger due to the expansion of the PEG chains from the core surface of the micelle to the solution, so the sizes of the micelles in water are larger than those in dry state.

#### Thermostability of the PSF-*b*-PEG Micelles

Spherical micelle solutions prepared using PSF-*b*-PEG with different block ratios (PEG content: 47%, 31%, 21%, and 14%, respectively) were diluted several times and dropped on cleaned silicon wafers. Then the silicon wafers were placed in a vacuum drying oven at heated temperatures for 30 min. The samples were used for SEM tests, and the high temperature resistance of the micelles was evaluated by observing the change of the sample morphologies. The SEM images are shown in Figure 8. It can be seen from the images that with the decrease of PEG content, the high temperature resistance of micelles increases. The spherical micelles prepared using 47%-PEG-content PSF-*b*-PEG (FG-4) became completely viscous flow state at 150 °C after 30 min. But the morphology of spherical micelles prepared using PSF-*b*-PEG with 21% PEG content (FG-2) can keep unchanged

under the same condition. The main reason is that the increase of PEG content leads to the decrease of glass transition temperature and viscous flow temperature, so the larger the PSF ratio is, the better the high temperature resistance of the micelles is. When the temperature increased to 180 °C, the micelles basically collapsed and even adhered to each other and lost their regular spherical features at 200 °C. As mentioned above, it can be roughly judged that the prepared PSF-*b*-PEG spherical micelles should be able to withstand a temperature of 150–180 °C. In contrast, PS-*b*-P2VP spherical micelles became unstable when subjected to thermal treatment at 150 °C for 30 min (Supporting Information, Figure S3). These results demonstrated that the PSF-based micelles were more thermally stable than the PS-based micelles. The PSF-*b*-PEG micellar spheres with higher thermostability are expected to be applied in demanding environmental conditions such as heating involved surface modification process.<sup>27</sup>

#### CONCLUSIONS

Spherical micelles are successfully prepared by direct dissolution method using PSF-*b*-PEG. TEM results show that the PSF-*b*-PEG spherical micelles are core-shell structures with PEG as the corona and PSF as the cores. By analyzing the DLS curve and SEM images, the particle sizes of PSF-*b*-PEG spherical micelles prepared with AA as solvent are both uniform in wet and dry state, and the particle sizes of the micelles in wet state are larger than those in dry state, as a result of the PEG corona chain segment stretches in aqueous solution. Temperature shows an important influence on the formation of micelles. There is a critical temperature below which the micelles could not form. In general, the diameters

of the micelles increase with the increase of temperature. When the external conditions are the same, the diameters of the micelles decrease with the decrease of PEG contents. For PSF-*b*-PEG with definite structures, the concentrations of the solution also affect the micelle sizes. With the increase of solution concentrations, the micelle sizes increase firstly, then decrease, and gradually tend to a stable value. Moreover, the experiments of high temperature resistance and dispersivity in water are carried out, which make possible the applications in demanding environmental conditions such as heating involved surface modification process.

#### ACKNOWLEDGMENT

Financial support from the National Basic Research Program of China (2015CB655301), Natural Science Foundation of China (21776126), the Jiangsu Natural Science Foundation (BK20150063), and the Program of Excellent Innovation Teams of Jiangsu Higher Education Institutions is gratefully acknowledged.

#### REFERENCES AND NOTES

- 1 C.-Y. Sun, S. Shen, C.-F. Xu, H.-J. Li, Y. Liu, Z.-T. Cao, X.-Z. Yang, J.-X. Xia, J. Wang, *J. Am. Chem. Soc.* **2015**, *137*, 15217.
- 2 K. Cui, X. Lu, W. Cui, J. Wu, X. Chen, Q. Lu, *Chem. Commun.* **2011**, *47*, 920.
- 3 Y. Bae, S. Fukushima, A. Harada, K. Kataoka, *Angew. Chem. Int. Ed.* **2003**, *42*, 4640. S4640/4641-S4640/4611.
- 4 L. Zhang, A. Eisenberg, *J. Am. Chem. Soc.* **1996**, *118*, 3168.
- 5 R. K. O'Reilly, C. J. Hawker, K. L. Wooley, *Chem. Soc. Rev.* **2006**, *35*, 1068.
- 6 G. Riess, *Prog. Polym. Sci.* **2003**, *28*, 1107.
- 7 X. He, H. Liang, L. Huang, C. Pan, *J. Phys. Chem. B* **2004**, *108*, 1731.
- 8 M. W. Matsen, F. S. Bates, *Macromolecules* **1996**, *29*, 1091.
- 9 C. Vauthier, K. Bouchemal, *Pharm. Res.* **2009**, *26*, 1025.
- 10 M. Moffitt, K. Khougaz, A. Eisenberg, *Acc. Chem. Res.* **1996**, *29*, 95.
- 11 S. Krishnamoorthy, R. Pugin, J. Brugger, H. Heinzelmann, C. Hinderling, *Adv. Mater.* **2008**, *20*, 1962.
- 12 S. Krishnamoorthy, R. Pugin, J. Brugger, H. Heinzelmann, C. Hinderling, *Adv. Funct. Mater.* **2006**, *16*, 1469.
- 13 L. Zhang, H. Shen, A. Eisenberg, *Macromolecules* **1997**, *30*, 1001.
- 14 X. Yao, D. Chen, M. Jiang, *J. Phys. Chem. B* **2004**, *108*, 5225.
- 15 X. Yao, D. Chen, M. Jiang, *Macromolecules* **2004**, *37*, 4211.
- 16 Y.-H. Cho, J.-E. Yang, J.-S. Lee, *Mater. Sci. Eng. C* **2004**, *24*, 293.
- 17 L. Zhang, R. J. Barlow, A. Eisenberg, *Macromolecules* **1995**, *28*, 6055.
- 18 L. Zhang, A. Eisenberg, *Macromolecules* **1996**, *29*, 8805.
- 19 R. Wang, J. Peng, F. Qiu, Y. Yang, *Chem. Commun.* **2011**, *47*, 2787.
- 20 Z. Yang, Z. Wang, X. Yao, Y. Wang, *Langmuir* **2012**, *28*, 3011.
- 21 Z. Yang, Z. Wang, X. Yao, X. Chen, Y. Wang, *J. Membr. Sci.* **2013**, *441*, 9.
- 22 J. E. Mark, *Physical Properties of Polymers Handbook*, 2nd ed.; Springer Science: New York, **2007**.
- 23 J. Y. Park, M. H. Acar, A. Akthakul, W. Kuhlman, A. M. Mayes, *Biomaterials* **2006**, *27*, 856.
- 24 L. Wang, J. Wang, X. Gao, Z. Liang, B. Zhu, L. Zhu, Y. Xu, *Polym. Chem.* **2014**, *5*, 2836.
- 25 S.-W. Yeh, K.-H. Wei, Y.-S. Sun, U.-S. Jeng, K.-S. Liang, *Macromolecules* **2003**, *36*, 7903.
- 26 R. Nagarajana, K. Ganesh, *J. Chem. Phys.* **1989**, *90*, 5843.
- 27 D. Li, Y. Yan, H. Wang, *Prog. Polym. Sci.* **2016**, *61*, 104.